

Petrogenesis of Fe-Ti oxides in amphibole-rich veins from
the Lherz orogenic peridotite (Northeastern Pyrénées,
France)

Jean-Pierre LORAND and Michel GREGOIRE

1 Laboratoire de Minéralogie et Cosmochimie, Muséum National d'Histoire Naturelle et CNRS
UMR 7202, CP 52, 61 Rue Buffon, 75005 Paris, France (jplorand@mnhn.fr)

2 CNRS UMR 5562-OMP, Toulouse University, 14 Av. Edouard Belin, F-31400 Toulouse, France

Abstract : Accessory, homogeneous ilmenite and rutile are important oxide phases in amphibole-rich high-pressure cumulate veins which crosscut the Lherz orogenic lherzolite massif. Those veins crystallized from alkaline melts at $P = 1.2\text{-}1.5$ GPa within the uppermost lithospheric mantle. Transitional basalts contaminated by peridotitic wall-rocks and then uncontaminated alkali basalts (basanites) reused the same vein conduits. Petrographic observations give evidence that Fe-Ti oxide saturation depends on the silica contents of each parental melt. The water-poor silica-rich transitional melts that generated websterites and plagioclase-rich clinopyroxenites reached early Ti-oxide saturation (1200°C ; 1.5 Gpa). Rutile is as abundant as ilmenite. It is enriched in Nb-Zr-Hf by a factor of 10 to 100 relative to either amphibole or ilmenite. The amphibole pyroxenites and hornblendites crystallized from basanites reached late Fe-Ti oxide saturation after precipitation of amphibole, with ilmenite crystallizing along with phlogopite in the latter. The Lherz ilmenites are devoid of exsolution and contain very little trivalent iron. This compositional feature indicates more reducing crystallization conditions than usually inferred for alkali lavas and their megacrysts (FMQ \pm 1). The veins incompletely equilibrated for redox conditions with their wall-rock peridotites which record more oxidizing conditions (FMQ \pm 1). The veins also exchanged magnesium and chromium, as suggested by Cr-bearing, Mg-rich ilmenite (up to 44 mol% MgTiO_3) in veins less than 3-4 cm thick. Mg-rich ilmenite megacrysts occurring in alkali basalts could be actually xenocrysts from veins similar in thickness to those occurring at the Lherz massif, although crystallized from more oxidized magmas.

I - INTRODUCTION

Mg-rich ilmenite megacrysts are characteristic feature of diamondiferous kimberlitic lavas while ilmenite and rutile are major minerals in mica-amphibole-rutile-ilmenite-diopside (MARID) nodules, thought to be generically related to kimberlitic fluids (Mitchell, 1978; Haggerty et al., 1979; Haggerty and Tompkins, 1984, Grégoire et al., 2002; Wyatt et al., 2004 and references therein). Compared to cratonic mantle sampled by kimberlites, Fe-Ti oxides are not normal component of the shallow upper mantle source of basalts. This is suggested by the scarcity of ilmenite megacrysts in continental lavas (Irving and Frey, 1984; Wilkinson and LeMaître, 1987). Ilmenite was occasionally reported in areas affected by mantle metasomatism of the Fe-Ti type (Menzies and Hawkesworth, 1987). Rutile was identified as important repository of high-field strength elements (HFSE), which may account for some decoupling between HFSE and other incompatible trace elements, in migrating metasomatic melt/fluids (Bodinier et al., 1996; Ionov et al., 1999; Grégoire et al., 2000a, b; Moine et al., 2001; Kalfoun et al., 2002). Both oxides are intimately associated with hornblendite vein systems. However, compared to major minerals, Fe-Ti oxide have not been studied in detail, especially as regard to the timing of Fe-Ti oxide precipitation with respect to other metasomatic minerals and the conditions that favour either ilmenite or rutile are unclear.

The Lherz orogenic lherzolite massif (Eastern French Pyrenees) displays the best occurrence of amphibole pyroxenites and hornblendites veins exposed in a sub-continental lithospheric mantle (Conquéré, 1971; Fabriès et al., 1991). These veins display a great variety of rock types and their major constituent minerals (clinopyroxene, amphibole) are compositionally similar to mafic megacrysts sampled by alkali basalts (Bodinier et al., 1987; Fabriès et al., 2001 and references therein). Moreover, unlike xenoliths and xenocrysts from alkali basalts, the amphibole-rich veins from orogenic massifs display their original structural relationships within the

lithospheric upper mantle on a metric scale. It is therefore possible to determinate accurately the crystallization order of the Fe-Ti oxides with respect to the surrounding silicates.

The present paper provides results from a comprehensive investigation of the 23 reference samples studied by Bodinier et al. (1987), Downes et al. (1991) and Fabriès et al. (2001). Each sample was studied with reflected light microscopy and the Fe-Ti oxides analysed with an electron microprobe. High-field strength elements (Ti, Zr, Hf, Nb, and Ta) were analysed in-situ by laser-ablation ICPMS in one specific sample to assess the origin of rutile. Mineralogical and geochemical features of Fe-Ti oxide assemblages are interpreted in the light of the petrological framework previously discussed for the Lherz amphibole-rich veins by Bodinier et al. (1987) and Fabriès et al. (2001). As the saturation of a silicate melt with respect to Fe-Ti oxides strongly depends on its silica activity (Green and Pearson, 1986; Cawthorn and Biggar, 1993; Xiong et al., 2005; Klemme et al., 2006), Fe-Ti oxides could be good markers of the degree of contamination by wall-rock peridotites of each parental melt that circulated in the Lherz vein conduits. Those veins allow to reassess the mechanism producing the Mg-rich ilmenite -either magnesian basalts precipitating Mg-rich ilmenite as primary magmatic phase or resulting Fe-Mg exchange reactions between veins and peridotite wall-rock- That issue was not clarified by the previous studies of the few occurrences of Mg-rich ilmenites occurring in nodules from continental alkali basalts (Leblanc et al., 1982; Hörnig and Wörner, 1991; Grégoire et al., 2000a). Fe-Ti oxides also provide important information on the oxygen fugacity controlling the Fe-Ti metasomatism of the subcontinental-upper mantle.

II - Petrography and petrogenetic features of the Lherz amphibole-rich veins

The orogenic peridotite massif of Lherz, Eastern Pyrenees, is composed of spinel lherzolites enclosing >10 m thick harzburgitic lenses (Fig. 1 in Le Roux et al., 2007). Centimetre- to dm-thick

spinel websterites and rare garnet pyroxenites define a layering within the peridotites. All these peridotites and pyroxenites display coarse-granular to porphyroclastic textures which result from two superimposed deformation-recrystallization stages (Conqu  r   and Fabri  s 1984a; Fabri  s et al. 1991; Le Roux et al., 2007). The coarse granular texture was generated by an early recrystallization stage at about 950  C and 1.2-1.5 GPa (D1-R1). A second episode of high-stress, shearing deformation (D2) generated the porphyroclastic texture and a foliation at P between 1.3 and 0.8 GPa and $T \leq 950^\circ\text{C}$ (V  til et al. 1988).

The amphibole-rich veins crop out in seven zones referred to as “injection zones” in Fabri  s et al., (2001). In zones A, B, C, and D, investigated in the present study (see Fig. 1 in Fabri  s et al., 2001) about 15 to 20 sub-parallel veins are gathered over a few square meters, often intruding the contact between lherzolites and harzburgitic bands. Each vein ranges in thickness between 3 and 30 cm. They intruded the peridotites during the D2-R2 plastic flow (see V  til et al. 1988). According to ^{39}Ar - ^{40}Ar and Sm-Nd model ages, the Lherz amphibole-rich veins are high-pressure cumulates from the mid-Cretaceous alkaline magmatism in the North Pyrenean Zone (Fabri  s et al., 1991; Downes et al., 1991). This magmatism is independent from mantle plume (Azambre et al., 1992). It rather derives from an enriched subcontinental lithosphere contaminated by terrigenous continental sediments (Downes et al., 1991; Mukasa et al., 1991).

The petrogenesis of Lherz amphibole-rich veins was thoroughly discussed by Fabri  s et al. (2001) who defined five paragenetic end-members, in addition to hornblendites: spinel orthopyroxenite, amphibole websterite, amphibole ariegite, amphibole garnet ariegite, and amphibole garnet clinopyroxenite. *Ariegites* represent a mantle rock-type defined in the Lherz massif by Lacroix in 1901 and correspond to pyroxenites that contain clinopyroxene, orthopyroxene and spinel (Cr-free spinel-hercynite solid solution) as early cumulus phases; Cr-free, pyrope-rich (50  4 mole %) garnet containing about 13 mole % grossular component and K₂O-poor pargasite, the latter replacing clinopyroxene are late-magmatic minerals. *Amphibole ariegites* are

composed of clinopyroxene + spinel \pm orthopyroxene \pm amphibole. *Garnet-bearing amphibole ariegites* differ in that garnet coexists with spinel (up to to 20 vol. % in the garnet-rich amphibole ariegites). In veins more than \sim 10 cm-thick, the outer zone is amphibole ariegite whereas the center of the veins is occupied by garnet-rich amphibole ariegite or clinopyroxenite. According to Fabriès et al. (2001), clinopyroxene compositions are similar to megacrysts from alkali basalts and clinopyroxenes synthesized at high pressure (1.3-1.8 GPa) from transitional basalt composition. However, Al enters mostly octahedral sites (Al^{VI}/Al^{IV} ratios > 1), mainly combined with Na in a jadeitic substitution. The alkaline affinity of the parental melt is corroborated by high LREE abundances in whole-rock and mineral separates ($La_N = 90$ to 230 ; $La_N/Yb_N = 15-20$; N: chondrite-normalized; Bodinier et al., 1987) and Sr-Nd-Pb isotopic compositions (Downes et al. 1991; Mukasa et al. 1991; MacPherson et al. 1996). *Garnet amphibole clinopyroxenite* comprises augitic clinopyroxene, amphibole and garnet porphyroclasts commonly containing rutile inclusions.

In injection Zone D, the veins are amphibole-poor pyroxenites belonging to two specific petrographic types: i) *Amphibole websterites* and ii) *garnet plagioclase amphibole clinopyroxenite*. Amphibole websterites occur as two thin amphibole-poor dikes (≤ 5 cm thick) showing in order of decreasing abundance, clinopyroxene, orthopyroxene, amphibole and spinel (Table 1). The garnet plagioclase amphibole clinopyroxenite (sample 71-334) occupy the margins of a 30 cm-thick vein enclosing an amphibole-poor garnet clinopyroxenite core (average grain-size of 2-5 mm). The most distinctive feature of sample 71-334 is the unusual abundance of albite-rich (An_{17-20}) plagioclase which may represent 5 to 10 % of the modal composition whereas amphibole is a late-crystallizing minor phase (<5 %).

Amphibole pyroxenites contain hornblendite pockets isolating amphibole pyroxenite septa of all size. Hornblendites may also occur as swarms of randomly oriented dikelets, a few mm- to 5 cm-thick, frequently cross-cutting each other, or bifurcating, coalescing and forming an anastomosing network. A largely undeformed lenticular hornblendite pocket, up to 40 cm across,

made from interlocked red brown kaersutite large crystals, up to 4 x 2 cm, that are almost devoid of kink bands or undulating extinction also occurs. Reddish-brown titanian phlogopite (≤ 15 vol %; $\text{TiO}_2 = 6.2 - 8.9$ wt%; $\text{Mg\#} > 0.75$; $\text{Mg\#} = \text{Mg}/(\text{Mg} + \text{Fe}_{\text{total}})$) occurs mainly interstitial to the kaersutite large crystals or along its cleavage planes. Kaersutite and intercumulus phlogopite are crystalline segregates from primary ($\text{Mg \#} = 0.6$; 4-6 wt% H_2O) basanite (10.6 wt% average normative nepheline; Fabriès et al., 2001). The trace element composition of the hypothetical liquids in equilibrium with hornblendites display marked enrichment of LREE and fractionation of HREE with $(\text{La}/\text{Yb})_{\text{N}}$ in the range 15-20 (Bodinier et al., 1987).

Fabriès et al (2001) provided strong evidence that hornblendites are not direct fractionation products from the parental magmas of amphibole pyroxenites. They shown that transitional basalts and then basanitic melts, mostly reusing the same vein conduits, were produced within a restricted time span of approximately 5 My (between 105 and 100 My ago) from the same mantle source (Downes et al. 1991), characterized by high ϵ_{Sr} (+5.7 to +7.0), and low ϵ_{Nd} (-22 to -26; see also Woodland et al., 1996). A continuous process of melting or melt-rock interaction affected the lithospheric mantle beneath the North Pyrenean Zone (NPZ) during the mid-Cretaceous. The transitional basalt composition is the end-product of extensive dissolution of orthopyroxene from wall rock peridotite by low-grade alkaline melts produced at the MBL/TBL transition zone (about 45-50 km deep). These reactions generated 2-3 mm-thick zones of anhydrous spinel orthopyroxenites at the margins of most amphibole-rich veins, while increasing Cr content in spinels, clinopyroxenes and kaersutites toward the vein margins. Zone-D pyroxenites are assumed to have crystallized from the most contaminated transitional basalt under low-water pressure as inferred from the low amphibole modal abundance. Assimilation of opx by opx-undersaturated melts can indeed produce very silica rich melts (Zinngrebe and Foley, 1995; Shaw et al., 1998). Continuous fluid ingress allowed remelting of the deeper veined mantle to produce volatile-rich basanitic melts that precipitated hornblendites (Fabriès et al., 2001).

III Petrography of Fe-Ti oxide mineral assemblages

Modal abundances of Fe-Ti oxides were estimated by a least-square regression from bulk-rock analyses (Bodinier et al., 1987) and mineral compositions (Fabriès et al., 2001). Amphibole ariegite veins containing amphibole-rich zones are devoid of Fe-Ti oxides or only display a few grains in each polished thin section. Nevertheless, Fe-Ti oxides always occur in the peridotite wall rock, over a distance of several centimetres away from the vein margins. These oxides are commonly observed near Cr-Al spinel and/or enclosed within olivine. Fe-Ti oxides are accessory minerals in most amphibole and garnet-bearing ariegites and clinopyroxenites (0.5-1 wt. %). An overall Fe-Ti oxide enrichment (up to 4 ± 2 wt. %) is observed in Zone-D pyroxenite veins that are markedly poorer in amphibole (Table I).

Ilmenite is the predominant oxide phase and occurs in all of the amphibole-rich veins. When ilmenite is the only oxide, it occurs as discrete intergranular grains ranging in size from a few μm to mm-sized crystals. Anhedral to regularly faceted ilmenite inclusions occur in kaersutite, garnet, olivine and plagioclase but are lacking or very rare in the early liquidus mineral phases (clinopyroxene, spinel and orthopyroxene).

Intergranular ilmenite grains are anhedral and display scalloped grain boundaries. They are commonly observed near the kaersutite porphyroclasts but many grains are dispersed within the fine grained matrix. All ilmenite grains are homogeneous. They may display deformation textures (undulating extinction, kink banding; Fig. 1A). Some polycrystalline aggregates of ilmenite grains with triple junctions meeting at 120° may sometimes occur; (Fig. 1B). Many grains are also fractured. The fractures planes cross-cut neoblast grain boundaries and therefore appear to postdate plastic deformation. Ilmenite underwent local and slight deuteric alteration into titanite + hematite.

In addition of being richer in Fe-Ti oxides, Zone-D amphibole pyroxenites show abundant primary rutile. Rutile is by far more abundant at the margins of the veins than towards the centre. Sample 71-334, the thickest veins (30 cm) display a mineral zonation marked by abundant ilmenite + rutile (with rutile predominating over ilmenite) grains over a distance of 1-2 cm from the vein margins whereas the centre of the vein only contains ilmenite. Rutile may form 200 µm large primary crystals included in amphibole, along cleavage planes of orthopyroxene and clinopyroxene or interstitial between the silicates. Discrete rutile is commonly adjacent to Al-rich spinel. Rutile and ilmenite may occur as isolated grains or forming two-phase assemblages either dominated by rutile or ilmenite (Fig. 1D). Nevertheless, two-phase oxide grains with 50 % ilmenite / 50 % rutile are common (Fig. 1C).

Rutile also appears in a few hornblendite dikes, yet in subordinate amount compared to ilmenite and never as coarse isolated grains. These rocks are of particular interest because primary magmatic textural relationships between oxide and silicate phases are better preserved, due to a lower degree of plastic deformation. Kaersutite megacrysts are surrounded or cross-cut by chains of ilmenite + rutile + phlogopite along fracture planes (Fig. 1E). Furthermore, these chains penetrate the basal cleavage planes of kaersutite, are necked-down and may give rise to negative crystal-shaped inclusions in the kaersutite. The large, inequigranular interstitial ilmenites have ragged boundaries which penetrate euhedral Ti-phlogopite crystals (Fig. 1F). All these textural features suggest that the Fe-Ti oxides crystallized after kaersutite and at the same time or after phlogopite.

IV Mineral chemistry

Major element contents of the minerals were determined with the Cameca Camebax fully automated electron microprobe of the «Muséum National d'Histoire Naturelle" in Paris. The electron microprobe was operated with 15-kV accelerating voltage, sample current of 10 nA, a

beam diameter of 2–3 mm, with natural (wollastonite, rutile, albite, forsterite, rhodonite, K feldspar, hematite) and synthetic minerals (Mn_2O_3 , Cr_2O_3 , NiO) as standards. Count times were 10 s/peak, 10 s/backgrounds. Detection limits range between 0.01 and 0.05 wt%. $\text{Fe}^{3+}/\text{Fe}^{2+}$ ratios have been calculated according to the Finger (1972) method to satisfy stoichiometry. Lucas et al. (1989) and Wyatt et al. (2004) provided evidence that this method is useful, provided that ilmenite composition belongs to the simple system $\text{Fe}^{2+}\text{-Mg-Ti-Fe}^{3+}$ and no element other than Fe is in more than one oxidation state. According to Mössbauer studies (Virgo et al., 1988), EMPA corrected data provide an upper bound of the trivalent iron content.

Some transition elements (V, Co, Ni) and the high field strength (Zr, Hf, Nb, Ta) trace element contents of ilmenite and rutile were determined by LAM-ICPMS (University of Cape town) in one Zone-D amphibole websterite (74-270), following the technique described by Grégoire et al. (2001). That sample is representative of the amphibole-poor samples containing coarse-grained rutile, associated with ilmenite. Analyses of more ilmenite-rutile pairs were difficult in hornblendites because of rutile grain size ($<50\mu\text{m}$) and its complex intergrowths with ilmenite.

Major elements

Ilmenite is devoid of chemical zoning. Its MgTiO_3 content varies in parallel to the bulk rock mg ratio ($100 \times \text{Mg}/\text{Mg} + \text{Fe}_{\text{total}}$) which is dependent on the thickness of the veins (Fig. 2). Ilmenite in the thinnest amphibole websterite veins and hornblendite dikes (< 4 cm thick) contain up to 44 mole % MgTiO_3 and compositional variations from grain to grain are moderate (Table 2). Such magnesian compositions compare well with those of Mg-rich ilmenite megacrysts from the Tahalra alkali basalts (Hoggar, Algeria; Leblanc et al., 1982) and those of the zirconolite-bearing ilmenite ultrapotassic veins from the Mt Melbourne volcanic field (Australia; Hornig et al, 1991). Our Mg-rich ilmenites are also similar to kimberlitic ilmenites, except for their lower Al_2O_3 (< 0.1 wt %) and Cr_2O_3 (< 0.3 wt %) contents.

Lherz ilmenites nevertheless are distinct from both kimberlitic ilmenites and alkali basalt hosted ilmenite megacrysts by their very low Fe₂O₃ contents (0-5 wt. %; Figs 3). Hence, Pyrenean Mg-ilmenites plot in an area of the FeTiO₃-MgTiO₃-Fe₂O₃ ternary diagram where there are very few terrestrial occurrences (Fig. 4). Similar Fe³⁺-poor Mg-rich ilmenite occurs as intergrowth with diamonds (Sobolev et al. 1971; Sobolev, 1974; 1984), as on-craton kimberlite megacrysts (Wyatt et al., 2004) and in rutile-bearing amphibole rich veins cross-cutting mantle peridotites (Cornen et al., 1999; Moine et al., 2001). Fe³⁺-poor highly magnesian ilmenites (up to 60 mol.% MgTiO₃) were also reported from millimetre-thick K-feldspar + Cr-spinel + rutile + armalcolite + ilmenite metasomatic veins from several peridotite xenoliths worldwide (Ionov et al., 1999; Grégoire et al., 2000; Fig. 3).

In the veins more than 4 cm thick, ilmenite contains less than 20 moles % MgTiO₃ and plots near to or within the field of basic rocks in the FeTiO₃-MgTiO₃-Fe₂O₃ ternary diagram (Fig 4). It is slightly Fe₂O₃-richer than the Mg-ilmenites; some data overlap the lower Fe³⁺ bound of ilmenite megacrysts from alkali basalts (Fig. 3). Ilmenite inclusions in subsolidus plagioclase are much less magnesian (< 7 mole % MgTiO₃) than intergranular ilmenites surrounded by Fe-Mg silicates (Fig. 4, Table III). Such a relationship suggests that the composition of the silicates controls the ilmenite chemistry (see below).

Ilmenite displays compositional variations as a function of the distance from the vein margins, as previously noted by Bodinier et al. (1987) and Fabriès et al. (2001) for silicates coexisting with ilmenite. In Zone-D plagioclase clinopyroxenite vein (Fig. 5), the geikeilite content decreases sharply from 39 to 17 mol. % over a distance of 1.5 cm from the vein wall, thus reproducing the evolution of the silicate mg numbers (see Fig. 5 in Fabriès et al., 2001). At about 2 cm from the vein wall, the geikeilite contents are similar to those of the other thick veins. Ilmenite grains occurring in the peridotite wall rocks of the amphibole-rich veins display similar compositional trends to those of the veins (table II). They are highly magnesian (30 moles%

MgTiO₃) when hosted by massive harzburgites (Fo91) and Mg-poorer (<16 mol. % MgTiO₃) when occurring within thin Fe-rich peridotites (Fo75) interlayered between thick amphibole-pyroxenite veins (Table II).

Chromium contents vary in a similar way as MgO, both within a single vein or from one vein to another. Taken as a whole, analyses of Lherz ilmenite define a rough positive correlation between MgO and Cr₂O₃ (Fig. 6). Chromium was systematically detected in Mg-rich ilmenites (0.16-0.30 wt. % Cr₂O₃) whereas it is generally below detection limits (<0.05wt. % Cr₂O₃) in MgO-poor ilmenites.

Trace element contents.

Ilmenite contains significant amount of V, Co and Ni but rutile only contains significant amount of V. Ilmenite displays a lower HFSE content than those of rutile but can have sometimes a relatively high Ta content (Table IV). The ilmenite analysed at the contact zone between the vein and host peridotite and close to a rutile grain is higher in Ni (1105-1195 ppm) and Co (120-150 ppm) and lower in Nb (1-2 ppm), Ta (0.20-0.25 ppm) and slightly lower in Zr (15-25 ppm) and Hf (0.30-1 ppm) for a similar V (110-230 ppm) than those occurring in the peridotite wall-rock and far from a rutile grain (Ni: 195-750 ppm; Co: 45-105 ppm; V: 180-310 ppm; Nb: 30-45 ppm; Ta: 4-10 ppm; Zr: 25-35 ppm; Hf: 2 ppm). The rutile occurring in the core of the vein is high in Zr (1485-1610 ppm), Nb (~ 1100 ppm) and Ta (65-90 ppm) and slightly high in Hf (~ 35 ppm). Finally the one occurring at the vein/host peridotite contact zone displays similar Zr (1490 ppm) and Hf (32 ppm) contents but is much lower in Nb (180 ppm) and Ta (4 ppm).

V. Discussion

VA The order of crystallization of ilmenite and rutile: a benchmark of silica activity.

Petrographic observations give evidence that Fe-Ti oxides did not precipitate at similar stage of the crystallization of the Lherz amphibole-rich veins. Ilmenite crystallized late, i.e. contemporaneous to kaersutite in the amphibole-rich pyroxenites (ariegite, clinopyroxenites). The few clinopyroxene-hosted ilmenite inclusions in those rocks are clearly of secondary origin, because they are commonly surrounded by a thin (10-30 μm thick) kaersutite rim suggesting reactions between pockets of differentiated Ti-rich melt and the host clinopyroxene rather than primary entrapment of early liquidus ilmenite. Kaersutite-ilmenite textural relationships in the hornblendites argue for late ilmenite precipitation, simultaneously with Ti phlogopite. By contrast, rutile and ilmenite that are enclosed in pyroxenes and amphibole from Zone-D amphibole-pyroxenites are early crystallizing phases, predating amphibole and contemporaneous to pyroxenes. For the sake of the discussion, samples from this zone will be treated separately.

Experimentally determined crystallization temperatures of ilmenite never exceed 1120°C at atmospheric pressure in the $f\text{O}_2$ range FMQ-NNO (Thompson, 1976; Cawthorn and Biggar, 1993). Ti-pargasite may be stable up to 1150°C at 1.0 GPa, but only under water-saturated conditions (e.g. Gilbert et al, 1982). For water activity below 1, Ti-pargasite does not crystallize above 1000-1050°C while cpx, along with spinel are stable at about 1230-1250°C over the pressure range 0.6-1.4 GPa (Upton and Thomas, 1980; Véttil et al, 1988 ; Fabriès et al., 2001). This suggests that ilmenite precipitated at about 200°C below the liquidus of the amphibole-rich pyroxenites and close to the solidus for the hornblendite veins (<1000°C; Conquéré, 1971). This late crystallization of ilmenite is well accounted for by experimental studies of Fe-Ti oxides in natural basaltic compositions. Starting from MORB, continental flood basalts, alkali basalts and andesites, Green and Pearson (1986), Helz and Thornber (1987), Cawthorn and Biggar (1993) and Klemme et al. (2006) highlighted a positive correlation between crystallization temperatures of Fe-Ti oxides and melt TiO_2 contents; they also documented negative relationships between the TiO_2 content necessary for the melt to reach the Fe-Ti oxide saturation and the silica content. In other words, for

melts of similar TiO₂ contents, Ti-rich oxides are more soluble in SiO₂-poor compositions (i.e. alkali basalts) than in andesites because of the polymerizing effect of silica which reduces the number of octahedral sites available for the partitioning of Ti in the melt. Thus, the silica-undersaturated character of their parental alkali basalts was responsible for the late crystallization of ilmenite in the Lherz amphibole-rich pyroxenites (Fabriès et al., 2001). According to Helz and Thornber (1987) and Cawthorn and Biggar (1993), Hawaiian OIB and transitional olivine basalts of similar TiO₂ and SiO₂ contents than those of North Pyrenean alkali basalts (44-49.3 wt.% SiO₂; 3.0±0.5 wt.% TiO₂; Azambre et al, 1992; Fabriès et al., 2001), may dissolve up to 6 wt.% TiO₂ prior to be saturated with respect to ilmenite. Accepting this value for North Pyrenean alkali basalts, a Rayleigh fractionation model $C_i = C_{i0} \cdot F^{(D-1)}$ in which only Cpx incorporated significant amount of Ti ($D^{Ti}_{Cpx-liq.} = 0.47-0.38$; Hart, 1993) predicts ilmenite saturation for F=40%. The latter value is broadly consistent with Cpx modal abundances in the amphibole-rich pyroxenite veins (30-50 wt. %; Table 1). For the hornblendites the fact that ilmenite saturation was delayed until phlogopite crystallized likely results from the lower silica content (46.2 wt. %; Fabriès et al., 2001) of the parental alkali basalt compared with that of the transitional basalt that precipitated the amphibole-rich pyroxenite veins.

Regarding Zone-D pyroxenites, the primary origin of rutile, crystallized before or with ilmenite, is supported by in-situ analyses of HFSE systematic in 74 270 vein : rutile is greatly enriched in HFSE relative to both amphibole and ilmenite (a factor of 10 to 100 for Nb-Zr-Hf) while being not depleted in Cr and V relative to ilmenite. By contrast, the coexisting ilmenite is HFSE-depleted compared to amphibole ($D^{ilmenite-amphibole} < 1$; Fig. 8). Magmatic rutile (like rutile in 74 270 vein) shows a greater preference for Nb-Ta compared to ilmenite and pseudobrookite-armalcolite phases. Xiang et al (2005) reported rutile/melt partition coefficients $D_{Ta} = 129$; $D_{Nb} = 94$ vs. $D_{Zr} = 5.1$ and $D_{Hf} = 7.1$. For comparison, the Kd values for ilmenite-liquid or ilmenite-pseudobrookite are close to 1-5 for all four elements (Yang and Naslund, 2003; Klemme et al., 2006)

There are two evidences that parental melt to Zone-D amphibole-pyroxenites reached saturation with respect to Fe-Ti oxides at an earliest crystallization stage: i- primary rutile inside pyroxenes, concentrated at the margins of the veins, ii- much higher Fe-Ti oxide modal abundance. As suggested by the unusually high opx modal proportions (26 wt.%), the veins in Zone-D injection zone likely crystallized from the most SiO₂-rich liquids, resulting from the most advanced stage of peridotite opx assimilation by North Pyrenean alkali basalts. Moreover garnet plagioclase amphibole clinopyroxenite 71 334 crystallized from water-deficient melt because it is amphibole-poor (5 wt. %) and contains Na-rich magmatic plagioclases (Fabriès et al., 2001). By suppressing amphibole, the water-deficient conditions also enhanced early Fe-Ti oxide saturation in partitioning Ti into rutile and ilmenite. Xiang et al. (2005) experimentally demonstrated that water-poor Si-rich basaltic melts are required to precipitate rutile at $P > 1.5$ GPa.

The oxide assemblage of Zone-D amphibole pyroxenites (magnesian ilmenite + Nb-rutile) bear some similarities with rutile-bearing metasomatic K-feldspar veinlets documented in harzburgitic xenoliths from Kerguelen Islands, Mongolia and other provenances. In either case, like in Lherz Zone-D amphibole pyroxenite, Fe-Ti oxides crystallized from volatile-poor highly alkaline silicated small melt fractions that have extensively digested wall-rock opx (Ionov et al., 1999; Grégoire et al., 2000a). The latter authors invariably report minerals belonging to the armalcolite solid solution [(Fe Mg) Ti₂O₅]. Phase diagrams in the system FeO-MgO-TiO₂ indicate that the armalcolite solid solution [(Fe Mg) Ti₂O₅] cut across the tie-lines between rutile and Mg-rich ilmenites. Thus, two-phase oxide grains with 50 % ilmenite / 50 % rutile may actually be subsolidus decomposition products from previous armalcolite. This mineral did not survive the slow tectonic emplacement and cooling of the Lherz massif inside the crust because it decomposes into ilmenite and rutile at $T < 1010^{\circ}\text{C}$ at atmospheric pressure (Lindsley et al., 1974; Fig. 8). This temperature of decomposition goes up to 1100°C at 1 GPa and to 1200°C at 1.5 GPa (Friel et al., 1977). Hence, the maximum temperature for rutile co-crystallizing with ilmenite could be 1200°C ,

assuming 1.5 GPa of total pressure for the crystallization of the Lherz amphibole-pyroxenite magmatic veins.

VB Re-equilibration between oxides and peridotites and origin of high-Mg ilmenites.

As Mg and Ti have opposite behaviour during fractional crystallization, the large range of geikelite contents of Lherz ilmenites can hardly be reconciled with their crystallization from presumably Ti-rich but Mg-depleted evolved liquids. After crystallization of 50% or more of clinopyroxene, the MgO content in the silicate melt is expected to have fallen down below 4 wt. % (assuming Rayleigh fractionation and a $K_d^{\text{Fe-Mg}}_{\text{cpx-liq.}}$ of 0.25; Hart and Dunn, 1993). Ilmenite crystallizing from such differentiated liquids should contain ca. 5 wt. % MgO at best according to experimental studies (Green and Sobolev, 1975; Thompson, 1976; Cawthorn and Biggar, 1993). Such ilmenite compositions correspond to those analysed at Lherz in the core of the thickest amphibole-pyroxenite veins. By contrast, Mg-ilmenite compositions found at vein margins or in the thinnest (<4cm) veins testify to an overall Mg gain from neighbouring peridotites. Taken as a whole, relationships between ilmenite MgTiO_3 contents, the thickness of the amphibole-rich veins and the whole-rock mg numbers show that ilmenite was involved in the process of peridotite/melt interaction documented at Lherz between amphibole-rich veins and wall-rock peridotites (Bodinier et al., 1990; McPherson et al., 1996; Woodland et al., 1996; Fabriès et al., 2001). All these studies documented melt exchange from the vein to the surrounding peridotites over distance of tens of centimetres. For Fe-Ti oxides, dissemination over several centimetres inside wall-rock peridotites have been observed in some harzburgitic wall-rocks (Lorand et al., 1990). Porous flow propagation of alkali basalt within the solid peridotite matrix created advective currents which brought compatible transition elements (Mg, Ni, Cr) back to the amphibole-rich vein system (Bodinier et al., 1990). As chromium diffuses very slowly in the solid state compared to Mg (Freer, 1981), only a melt transport can account for the positive correlation between Cr and Mg in Lherz ilmenites. It

should be pointed out that, because Lherz ilmenite crystallized late, advective circulation of liquid should have been still efficient at high percentages of solidification in order to explain Mg-rich ilmenite intergrowths with phlogopite.

As suggested by their similar Mg ratio, ilmenites disseminated in the peridotites wall rocks and in the thinnest amphibole-rich veins reached equilibrium (Table II). However, within a single vein, there is evidence that ilmenite (like coexisting silicates) continued to exchange Fe-Mg at subsolidus temperatures. For example, ilmenite entrapped by subsolidus plagioclase is less magnesian than those adjacent to Fe-Mg silicates (clinopyroxene, kaersutite). Fabriès et al. (2001) pointed out that not only the early liquidus phases of the amphibole-rich veins (i.e. clinopyroxene, orthopyroxene and spinel) are Mg-enriched, but also the interstitial, subsolidus exsolution products such as olivine. Blocking temperatures for ilmenite can be estimated by the various equilibria involving mafic silicates (olivine, orthopyroxene, clinopyroxene) in the Lherz amphibole-rich veins. These latter have been modelled with the QUILF program (Andersen et al, 1993) for the three main pyroxenite parageneses (websterites, ariegites and clinopyroxenites), using our data coupled with mineral analyses of Fabriès et al. (2001). QUILF equilibration temperatures for ilmenite-olivine-orthopyroxene-clinopyroxene assemblages range from 650° to 730°C, i.e. 200° lower than those recorded by inter-silicate equilibration. Ilmenite is a minor phase disseminated in an infinite magnesium reservoir as represented by mafic silicates. It is also likely that Fe-Mg exchange reactions were enhanced by D2-R2 deformations that affected ilmenite, continuing down to ca. 750°C (Fabriès et al., 1991).

Our results shed some new light on the petrogenesis of Mg-rich ilmenites associated with Fe-Ti metasomatism in the shallow sub-continental mantle. Ti-rich evolved alkaline melt that extensively reacted with mantle peridotites can create suitable enrichment in both MgO and TiO₂. In agreement with our observations on Lherz amphibole-rich veins, all Mg-ilmenites so far reported from the shallow sub-continental upper mantle show centimetric grain size (<2 cm Leblanc et al.,

1982) or smaller (Hörnig and Wörner, 1991; Moine et al., 2001). The most magnesian ilmenites (up to 60 mol. % MgTiO₃) were reported from millimetre-thick K-feldspar + Cr-spinel + rutile + armalcolite + ilmenite metasomatic veins (Grégoire et al., 2000a; Fig. 3). In the latter case, highly modified alkaline melts have equilibrated with strongly refractory harzburgites (Mg number = 91-93; Grégoire et al., 2000a).

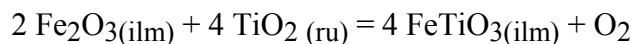
VC ilmenite composition and oxygen barometry results

The very low trivalent iron content is a distinctive feature of Lherz ilmenite compared to similar Mg-rich ilmenite megacrystals from kimberlites and alkali basalts (Figs 3 and 4). Moreover, these megacrystals invariably display titanomagnetite/spinel exsolutions ascribed to subsolidus reduction of the hematite end-member of the ilmenite solid solution (e.g. Leblanc et al, 1982; Haggerty and Tompkins, 1984; Haggerty et al, 1985). Although this mineral has been observed in samples from unknown location in one other Pyrenean peridotite massif (Freychinède; Lorand et al., 1990), titanomagnetite has not been identified in Lherz amphibole-rich veins, neither as discrete grains, nor as exsolution inside ilmenite, even in those showing microtextural evidence of deformation/recrystallization. Ilmenite included in silicates (plagioclase, garnet, kaersutite) and intergranular ilmenites that may have been in contact with deuteric fluids show very similar trivalent iron contents. An overall depletion in trivalent iron has also been noted by Fabriès et al. (2001) for major silicates (Fe^{3+}/Fe^{2+} atomic ratios_{CPX} ≤ 0.25 ; Fe^{3+}/Fe^{2+} atomic ratios_{AMPH} close to 0) and spinel ($Fe^{3+} < 0.055$ at. per formula unit) compared to clinopyroxene and amphibole megacrystals from alkali basalts. All these lines of evidence argue against significant modification of Fe^{3+}/Fe^{2+} ratio of Lherz ilmenites by subsolidus reduction and/or reequilibration with major minerals.

As titanomagnetite is lacking, the T-fO₂ values for Lherz amphibole-rich veins cannot be determined with the ilmenite-titanomagnetite geothermometer-oxybarometer (Buddington and

Lindsley, 1964). Thus, a-priori values of fO_2 were deduced from ilmenite isopleths (Frost and Lindsley, 1991): such isopleths are univariant curves that show the minimum fO_2 at a given temperature (c.f. Pasteris, 1985). These a-priori values were then used to deduce the T- fO_2 conditions for the assemblages involving ilmenite, orthopyroxene, clinopyroxene and spinel with the QUILF program (Andersen et al, 1993). In line with the hematite contents of ilmenite (Table III), our fO_2 estimation at 650-730°C range from FMQ-0.5±2 and FMQ-1±1 log units for two thin veins of garnet-poor amphibole ariegites (73-2B; 73-4), FMQ-4.7±1.3 and FMQ-3±0.3 for two thicker veins of garnet-rich clinopyroxenites (74-18 and 74-90) and for Zone-D amphibole-websterites. Note that where ilmenite is a trace phase (e.g. amphibole ariegites); the QUILF program generates large error bars, which make the fO_2 estimation debatable.

For Zone-D amphibole websterites, oxygen fugacity has also been estimated with the ilmenite (ilm)-rutile (ru) redox equilibrium



This was calibrated as an oxygen barometer for MARID nodules by Zhao et al. (1999).

Calculations were performed for 900°C and 1.5 GPa by using the equation

$$\log fO_2 = 22.59 - 25925/T - 3.09 \log T + 0.0016535P + 48.836P/T - 4 \log a_{\text{FeTiO}_3}^{\text{ilm}} + 4 \log a_{\text{TiO}_2}^{\text{Ru}} + 4 \log a_{\text{Fe}_2\text{O}_3}^{\text{ilm}} \text{ (Kbar; Kelvin),}$$

The analyses of Lherz ilmenite and rutile from Table II and ilmenite solid solution models of Ghiorso (1990) were also used. The value of $\log fO_2$ is within the range of estimations from the QUILF program (WM ±1 log unit; Fig. 9)

As expected from ilmenite compositional features, our fO_2 range extends to significantly lower values than those recorded by mafic megacrystals from alkali lavas, and MARID nodules in kimberlites ($fO_2 = \text{FMQ} \pm 1$ log unit; Leblanc et al., 1982; Sen and Jones, 1988; Haggerty and

Tompkins, 1984; Zhao et al., 1999; Fig. 9). It is also depressed compared to the fO_2 range calculated for Lherz peridotites using the spinel-olivine-orthopyroxene oxygen barometer (FMQ \pm 1 log unit; Woodland et al., 1992, 1996, 2006). The reduced nature of the amphibole-rich veins explains why harzburgitic wall-rocks of amphibole-rich veins do not display higher fO_2 compared to harzburgites sampled away from those veins (Woodland et al., 1996). The overall trivalent iron depletion of the minerals that constitute the amphibole-rich veins (including ilmenite) is reminiscent of a reduced parental magma that is not associated with mantle plume, such as North Pyrenean alkali basalts (Azambre et al., 1992). Thus, it also provides indirect support to Fabriès et al. (2001) suggestion of a redox-melting process for the genesis of North Pyrenean Cretaceous alkali basalts, as this model (Taylor and Green, 1986, 1989; Foley, 1988) assumes CH_4 -rich reduced fluids. By migrating upward through oxidized continental lithosphere, CH_4 oxidation releases water (+ graphite) which triggers low-degree melting of peridotitic vein walls. To date, pilot study of fluid inclusion in Lherz amphibole-rich veins has identified only high-density CO_2 -fluid included in garnet (Vétil et al., 1988). However, that fluid composition does not contradict the redox-melting model because: i) at $\log fO_2 = WM$, CO_2 is an important component in water-rich fluids (c.f. Andersen et al., 1984; Foley, 1988) and ii) fluid compositions now observed in Lherz amphibole-rich veins are residual after precipitation of the amphibole that incorporated all available water (Vétil et al., 1988). Such a composition also points out to partial reequilibration of Cretaceous alkali basalts during their upward migration through the oxidized lithospheric mantle now represented by Lherz peridotites.

Conclusion

Accessory ilmenite is a late-magmatic mineral in the Lherz amphibole-rich veins, except where parental alkali basaltic magmas have extensively reacted with wall-rock peridotites, thus

precipitating early ilmenite + rutile assemblages, perhaps as armalcolite at high temperatures and pressures of the upper mantle.

The rutile from the investigated veins represents a major HFSE reservoir in the upper mantle, in agreement with previous studies of rutile-bearing peridotites. However, this mineral is very subordinate compared to ilmenite. It requires peculiar conditions of low water activity, high silica activity and early TiO₂ saturation to crystallize from alkaline melts.

Advective melt transport from amphibole-rich veins and wall-rock peridotites account for coupled Mg-Cr enrichment in ilmenite. Such process can operate over a centimetric scale. By analogy with Lherz ilmenite, it is suggested that Mg ilmenite megacrysts from alkali basalts are disaggregated fragments from metasomatic veins that experienced similar Mg-Cr enrichment via melt/peridotite interaction.

Lherz ilmenite records lower f_{O_2} conditions in disequilibrium with the shallow subcontinental lithospheric mantle (FMQ \pm 1 log unit) represented by Lherz peridotites. The overall depletion in trivalent iron of the minerals that constitute the amphibole-rich veins (including ilmenite) is reminiscent of a reduced parental magma, ultimately generated by a redox-melting process of an enriched mantle source.

Acknowledgements

Financial support was provided by CNRS (UMR 7160). We dedicate this paper to our late colleague Prof. Jacques Fabriès who spent much time unravelling the petrogenesis of the Lherz amphibole-rich veins. The present version of the paper greatly benefited from comments of K-N Pang and Cliff Shaw; C. Ballhaus is warmly thanked for his editorial work.

References

Andersen DJ, Lindsley DH, Davidson PM (1993) QUILF: a Pascal program to assess equilibria among Fe-Mg-Mn-Ti oxides, pyroxenes, olivine, and quartz. *Computers and Geosciences*, 19:1333-1350

Andersen T, O'Reilly S Y, Griffin WL (1984) The trapped fluids phase in upper mantle xenoliths from Victoria, Australia: implications for mantle metasomatism. *Contrib Mineral Petrol* 88:72-45

Azambre B, Rossy M, Albarède F (1992) Petrology of the alkaline magmatism from the Cretaceous North-Pyrenean Rift Zone (France and Spain). *Eur J of Mineral* 4:813-834

Bodinier J-L, Fabriès J, Lorand J-P, Dostal J, Dupuy C (1987) Petrogenesis of amphibole-pyroxenite veins from the Lherz and Freychinède ultramafic bodies (Ariège, French Pyrenees). *Bull Mineral* 110:345-359

Bodinier J-L, Vasseur G, Vernières J, Dupuy C, Fabriès J (1990) Mechanisms of mantle metasomatism : geochemical evidence from the Lherz orogenic peridotite. *J Petrol* 31:597-628

Bodinier J-L, Merlet C, Bedini RM, Simien M, Reimaidi M, Garrido CJ (1996) Distribution of niobium, tantalum, and other highly incompatible trace elements in the lithospheric mantle: the spinel paradox. *Geochim Cosmochim Acta* 60:545-550.

Buddington AF, Lindsley DH (1964) Iron-titanium oxide minerals and synthetic equivalents. *J Petrol* 5: 310-357.

Cawthorn RG, Biggar G (1993) Crystallization of titaniferous chromite, Mg-rich ilmenite and armalcolite in tholeiitic suites in the Karoo Igneous Province. *Contrib Mineral Petrol* 114:221-235

Conquéré F (1971) Les pyroxénolites à amphibole et les amphibololites associées aux lherzolites du gisement de Lherz (Ariège ; France) : un exemple du rôle de l'eau au cours de la cristallisation fractionnée des liquides issus de la fusion partielle des lherzolites. *Contrib Mineral Petrol* 33 :32-61

Conquéré F, Fabriès, J (1984) Chemical disequilibrium and its thermal significance in spinel-peridotites from the Lherz and Freychinède ultramafic bodies (Ariège ; French Pyrenees). In : Kornprobst J. (ed) *Kimberlites II : The Mantle and Crust-Mantle Relationships*, pp. 319-332. Elsevier Science

Cornen G, Girardeau J, Monnier C (1999) Basalts, underplated gabbros and pyroxenites record the rifting process of the West Iberian margin. *Mineral Petrol* 67:111-142

Downes H, Bodinier J-L, Thirlwall M F, Lorand J-P, Fabriès, J (1991) REE and Sr-Nd isotopic geochemistry of Eastern Pyrenean peridotite massifs : Paleozoic sub-continental lithosphere modified by subsequent metasomatism? in "Orogenic Lherzolites and Mantle Processes", M.A. Menzies et al., (eds.) *J Petrol* pp. 97-116.

Fabriès J, Lorand J-P, Bodinier J-L, Dupuy C (1991) Evolution of the upper mantle beneath the Pyrenees during the Mesozoic : evidences from spinel lherzolite orogenic massifs. In "Orogenic Lherzolites and Mantle Processes", M.A. Menzies et al, (eds.). *J Petrol* pp. 55-76

Fabriès, J, Lorand J-P, Guiraud M (2001) Petrogenesis of mantle-derived amphibole-rich veins and relationships between amphibole-pyroxenites and hornblendites in the Lherz orogenic massif. *Contrib Mineral Petrol* 140:383-403

Finger LW (1972) The uncertainty in calculated ferric iron content of a microprobe analysis? *Carnegie Inst Wash, Yearbook* 71, 600-603

Foley SF (1988) The genesis of continental basic alkaline magmas : an interpretation in terms of redox melting. In « Oceanic and continental lithosphere; similarities and differences », M.A. Menzies and K.G. Cox (eds.). *J Petrol* 139-162

Freer R (1981a) Diffusion in silicate minerals and glasses : a data digest and guide to the literature. *Contrib Mineral Petrol* 76:440-454

Freer R (1981b) Interdiffusion studies in minerals with corundum structure : $Al_2O_3 - Cr_2O_3$. *Progress in experimental petrology, N E R C Publ Ser D*, 18:166-170

Frost BR, Lindsley DH (1991) Occurrence of iron titanium oxides in igneous rocks, In: Lindsley, D H (Ed.), *Oxide Minerals: Petrologic and Magnetic Significance; Reviews in Mineralogy*, 25, pp. 433-468

Friel J, Harker R I, Ulmer G C (1977) Armalcolite stability as a function of pressure and oxygen fugacity. *Geochim Cosmochim Acta* 41:403-410

Giorso MS (1990) Thermodynamic properties of hematite-giesselite-ilmenite solid solutions. *Contrib Mineral Petrol* 104:645-667

Green DH, Pearson NJ (1986) Ti-rich accessory phase saturation in hydrous mafic-felsic compositions at high P. *T. Chem Geol* 54 :185–201

Green DH, Sobolev NV (1975) Coexisting garnets and ilmenites synthesized at high pressures from pyrolite and olivine basanite and their significance for kimberlitic assemblages. *Contrib Mineral Petrol* 50:217-229

Grégoire M, Lorand J-P, O'Reilly SY, Cottin J-Y (2000a) Armalcolite-bearing, Ti-rich alkali veinlets and the budget of incompatible trace elements in some Kerguelen harzburgitic xenoliths. *Geochim Cosmochim Acta* 64 :674-693

Grégoire M, Moine BN, O'Reilly SY, Cottin J-Y, Giret A (2000b) Trace element residence and partitioning in mantle xenoliths metasomatized by Highly alkaline, silicate- and carbonate-rich melts (Kerguelen Islands, Indian Ocean). *J Petrol* 41: 477-509

Grégoire M, Bell DR, Le Roex AP (2002) Trace element geochemistry of glimmerite and MARID mantle xenoliths: their classification and their relationship to kimberlites and to phlogopite-bearing peridotites revisited. *Contributions to Mineralogy and Petrology*, 142:603-625.

Hart SR, Dunn P (1993) Experimental Cpx/melt partitioning of 24 trace elements. *Contrib Mineral Petrol* 113:1-8.

Haggerty SE, Hardie III RB, McMahon BM (1979) The mineral chemistry of ilmenite nodule associations from the Monastery diatreme. In : Boyd, F.R., Meyer, H.O.A., (eds). *The mantle sample. Proc. 2nd International Kimberlite Conference*, 2, pp. 249-256. Am. Geophys Union, Washington DC

Haggerty SE, Moore AE, Erlank AJ (1985) Macrocryst Fe-Ti oxides in olivine melilites from Namaqualand-Bushmanland, South Africa. *Contrib Mineral Petrol* 91:163-170

Haggerty S E, Tompkins L. A. (1984) Subsolidus reactions in kimberlitic ilmenites: Exsolution, reduction and the redox state of the mantle. In Kornprobst J. (ed) *Kimberlites 1 : Kimberlites and Related Rocks*, pp 83–105, Elsevier Science

Hörnig, I, Wörner G (1991) Zirconolite-bearing ultra-potassic veins in a mantle-xenolith from Mt Melbourne Volcanic Field, Victoria Land, Antarctica. *Contrib Mineral Petrol* 106:355-366

Ionov DA, Grégoire M, Ashchepkov I (1999) Feldspar-Ti oxide metasomatism in off-cratonic continental and oceanic upper mantle. *Earth Planet Sci Lett* 165 :37–44

Irving AJ, Frey FA (1984) Trace element abundance in megacrysts and their host basalts : constraints on partition coefficients and megacryst genesis. *Geochim Cosmochim Acta* 48, 1201-1227

Jang YD, Naslund HR (2003) Major and trace element variation in ilmenite in the Skaergaard Intrusion: petrologic implications. *Chem Geol* 193:109–125

Kalfoun K, Ionov D, Merlet C (2002) HFSE residence and Nb/Ta ratios in metasomatised, rutile-bearing mantle peridotites. *Earth Planet Sci Lett* 199: 49–65.

Klemme S, Gunther D, Hametner K, Prowatke S, Zack T (2006) The partitioning of trace elements between ilmenite, ulvospinel, armalcolite and silicate melts with implications for the early differentiation of the moon, *Chemical Geology*, 234:251-263

Leblanc M, Dautria J-M, Girod M (1982) Magnesian ilmenite xenoliths in a basanite from Tahalra, Ahaggar (Southern Algeria). *Contrib Mineral Petrol* 79:347-357

Le Roux V, Bodinier J-L, Tommasi A, Alard O, Dautria J-M, Vauchez A, Riches AJV (2007) The Lherz spinel ilmenite: refertilized rather than pristine mantle. *Earth Planet Sci Lett* 259:599-612

Lindsley DH (1991) Experimental studies of oxide minerals. In *Oxide minerals: Petrologic and Magnetic Significance* (ed. D. H. Lindsley). Mineral Soc Am Publ pp 61-88

Lindsley DH , Kesson SE, Hartzman S E (1974) The stability of armalcolite: Experimental studies in the system MgO-Fe-Ti-O. *Geochimica et Cosmochimica Acta*, Supplement 5, 1, 521–534.

Lorand J-P, Vétel J-Y, Fabriès, J (1990) Fe-Ti oxide assemblages of the Lherz and Freychinède amphibole-rich veins (French Pyrenees). First International Workshop on Orogenic Lherzolites and Mantle Processes, Blackwell Scientific publications, p. 31 (abstract).

Lucas H, Muggeridge M T, Mc Conchie (1989) Iron in kimberlitic ilmenites and chromian spinels: a survey of analytical techniques. In Ross et al., (eds.), *Kimberlites and Related Rocks*, Vol 1, Geol Soc of Austr. Spec Publ 14 pp. 311-322

MacPherson E, Thirwall M F, Parkinson I J, Menzies, M A, Bodinier J-L, Woodland A-B, Bussod, G (1996) Geochemistry of metasomatism adjacent to amphibole-bearing veins in the Lherz peridotite massif. *Chem Geol* 134:135-157

Menzies M A, Rogers N, Tindle A., Hawkesworth C J (1987) Metasomatic and enrichment processes in lithospheric peridotites, an effect of asthenosphere-lithosphere interaction. In : "Mantle metasomatism", M.A. Menzies and C.J. Hawkesworth eds. Academic press, London, 313-361.

Mitchell R H (1978) Geochemistry of magnesian ilmenites from kimberlites in South Africa and Lesotho. *Lithos* 10, 29-37.

Moine BN, Grégoire M, O'Reilly S Y, Sheppard S M, Cottin J-Y (2001) High Field Strength Element Fractionation in the Upper Mantle : evidence from amphibole-rich composite mantle xenoliths from the Kerguelen Islands (Indian Ocean). *J Petrol* 42:2145-2167

Mukasa S B, Shervais J W, Wilshire H G, Nielson J E (1991) Intrinsic Nd, Pb, and Sr isotopic heterogeneities exhibited by the Lherz alpine peridotite massif, French Pyrenees. In "Orogenic Lherzolites and Mantle Processes", M.A. Menzies et al, (eds.). *J Petrol* pp 117-134

Pasteris JD (1985) Relationships between temperature and oxygen fugacity among Fe-Ti oxides in two regions of the Duluth Complex. *Can Mineral* 23:111-127.

Sen G, Jones R E (1988) Exsolved silicate and oxide phases from clinopyroxenes in a single Hawaiian xenolith : implication for oxidation state of the Hawaiian upper mantle. *Geology* 16:69-72

Shaw CSJ , Thibault Y, Edgar AD, Llyod FE (1998). Mechanisms of orthopyroxene dissolution in silica-undersaturated melts at 1 atmosphere and implications for the origin of silica-rich glass in mantle xenoliths. *Contrib Mineral Petrol*, 132:354-370.

Simons B, Woermann E (1978) Iron titanium oxides in equilibrium with metallic iron. *Contrib Mineral Petrol* 66:81-89.

Sobolev NV (1984) Kimberlites of the Siberian platform : their geological and mineralogical features. In Glover J. and Harris D.G. (eds.) *Kimberlites occurrences and origin : a basis for conceptual models in exploration*. pp. 275-287. Geology department and University extension, University of Western Australia. publication n°8

Speidel DH (1970) Effect of magnesium on the iron-titanium oxides. *Amer J Sci* 268,:341-373

Taylor WR, Green DH (1989) The role of reduced C-O-H fluids in mantle partial melting. in Ross et al., (eds.), *Kimberlites and Related Rocks*, Vol 2, Geol Soc of Austr. Spec Publ n°14, pp. 593-602

Thompson R N (1976) Chemistry of ilmenites crystallized within the anhydrous melting range of a tholeiite andesite at pressure between 5 and 26 kbar. *Mineral Mag* 40:857-862

Upton B G J, Thomas JE, 1980. The Tugtutôq younger Giant Dyke Complex, South Greenland : fractional crystallisation of transitional olivine basalt magma. *J Petrol* 21:167-198

Vétil, J-Y, Lorand J-P, Fabriès J (1988) Conditions de mise en place des filons riches en amphibole du massif ultramafique de Lherz (Pyrénées Ariégeoises, France). C.R. Acad. Sci. Paris, série II, 307:587-593

Virgo D, Luth R W, Moats MA, Ulmer GC (1977) Constraints on the oxidation state of the mantle : an electrochemical and ^{57}Fe Mössbauer study of mantle-derived ilmenites. Geochim Cosmochim Acta 52:1781-1794

Wilkinson, J F G (1975) Ultramafic inclusions and high pressure megacrysts from a nephelinite sill, Nandewar Mountains, North-Eastern New South Wales, and their bearing on the origin of certain ultramafic inclusions in alkaline volcanic rocks. Contrib Mineral Petrol 51:235-262

Woermann E, Hirshberg A, Lamprecht A (1969) Das System Hämatit-Ilmenit-Giekelith unter hohen Temperaturen und hohen Drucken. Forts Mineral 47:79-80.

Wones DR, Gilbert MC (1982) Amphiboles in the igneous environment. In: Amphiboles: petrology and experimental phase relations (Edited by Veblin, D. R. et Ribbe, P. H.) pp 355-390. Reviews in Mineralogy 9B, Washington DC

Woodland A B, Kornprobst J, McPherson E, Bodinier J-L, Menzies MA (1996) Metasomatic interactions in the lithospheric mantle : petrologic evidence from the Lherz massif, French Pyrenees. Chem Geol 134:83-112

Woodland A B, Kornprobst J, Wood B J (1992) Oxygen thermobarometry of orogenic lherzolite massifs. J Petrol 33:203-230

Woodland A B, Kornprobst J, Tabit A (2006) Ferric iron in orogenic lherzolite massifs and controls of oxygen fugacity in the upper mantle. Lithos 89:222-241

Wyatt BA, Baumgartner M, Anckar E, Grutter H (2004) Compositional classification of “kimberlitic” and “non-kimberlitic” ilmenite. Lithos 77:819-840

Xiong X L, Adam T J, Green D H (2005) Rutile stability and rutile/melt HFSE partitioning during partial melting of hydrous basalt: Implications for TTG genesis. *Chem Geol* 218:339-359

Zhao D, Essene E J, Zhang Y (1999) An oxygen barometer for rutile-ilmenite assemblages: oxidation state of metasomatic agents in the mantle. *Earth Planet Sci Lett* 166:127-137

Zinngrebe E, Foley SF (1995). Metasomatism in mantle xenoliths from Gees, West Eifel, Germany: evidence for the genesis of calc-alkaline glasses and metasomatic Ca-enrichment. *Contributions to Mineralogy and Petrology* 122:79-96

Figure caption

Figure 1. Microphotographs of Fe-Ti oxides. A: intergranular ilmenite showing deformation twinning. B: Mosaic-recrystallized intergranular ilmenite. C: homogeneous ilmenite juxtaposed to clinopyroxene (amphibole ariegite). D: ilmenite-rutile (Ru) two-phase inclusion in clinopyroxene (74 270 amphibole-poor websterite) E: homogeneous ilmenite associated with amphibole. F: large intergranular ilmenite grain penetrated by phlogopite flakes (hornblendite).

Figure 2. Relationships between vein thickness, whole-rock Mg number and geikelite contents of ilmenite (mol. %).

Figure 3. MgO vs. TiO₂ diagram for the Lherz ilmenite (weight. %). Compositions of ilmenite megacrysts from alkali basalts are shown for comparison.

Figure 4. Plot of the Lherz ilmenite composition (mol. %) in the ternary diagram MgTiO₃ (geikelite)-FeTiO₃ (ilmenite)-Fe₂O₃ (hematite) contoured for fO₂ at 1300°C (Woermann et al., 1969). Fields for kimberlitic ilmenite and basic rocks from Mitchell (1978)

Figure 5. Variation of MgTiO₃ content of ilmenite (mol. %) as a function of distance from vein margins; Zone-D amphibole-poor plagioclase-clinopyroxenite vein (71-334).

Figure 6 : Chromium vs. magnesium diagram for Lherz ilmenite.

Figure 7. Compositional range of ilmenite coexisting with primary rutile in Zone-D amphibole-poor websterites. Note that, due to the extent of armalcolite solid solution, both minerals cannot coexist above 1010°C at 1 bar, or above 1200°C at 1.5 GPa (see text for more details).

Figure 8. Rutile/ilmenite, rutile/amphibole and amphibole/ilmenite partition coefficients for HFSE and some transition elements.

Figure 9. Oxygen fugacity estimates for the Lherz ilmenites (arrows) compared to ilmenite megacrysts in alkali lavas and experimental data.

SJ = ilmenite-clinopyroxene intergrowths in Hawaiian basalts (Sen and Jones, 1988); V = Virgo et al. (1977); H₇₉ = Haggerty et al., 1979 (Monastery ilmenites); H₈₅ = Haggerty et al (1985) (Namaqualand melilitic ilmenites); HT = Haggerty and Tompkins (1984) (Koidu kimberlitic ilmenites); L = Leblanc et al. (1982) (Tahala magnesian ilmenites; Algeria).

Experimental data: Th= Thompson (1976) ilmenite compositions with 0.1-0.13 at. % Fe³⁺ p.f.u. Sp and MgO = 3 wt. %): S: Speidel (1970) Mg ilmenite (10 wt % MgO, < 5 wt % Fe₂O₃); log fO₂ = -10.6 and T = 1160°C. K = Klemme et al. (2006) Fe³⁺-free Mg-rich ilmenites from transitional basalts at 1 GPa for oxygen fugacity = -11.6 at 1185°C and -11.45 at 1200°C).

Solid-solid oxygen buffer curves after Lindsley (1991)